Photochemistry and Photobiology, 2013, 89: 33–39

UV/TiO_2 Photocatalytic Degradation of Xanthene Dyes

Luciana Pereira*[1], Raquel Pereira[1], Catarina S. Oliveira[1], Laura Apostol[2], Mariana Gavrilescu[2], Marie-Noëlle Pons[3], Orfan Zahraa[3] and Maria Madalena Alves[1]

[1]IBB-Institute of Biotechnology and Bioengineering, Centre of Biologic Engineering, Minho University, Braga, Portugal
[2]Department of Environmental Engineering and Management, Faculty of Chemical Engineering & Environmental Protection, Gheorghe Asachi" Technical University of Iasi, Iasi, Romania
[3]Laboratoire Réactions et Génie des Procédés (UPR 3349 CNRS), Nancy University, INPL, Nancy Cedex, France

Received 28 April 2012, accepted 16 July 2012, DOI: 10.1111/j.1751-1097.2012.01208.x

ABSTRACT

UV/titanium dioxide (TiO_2) degradation of two xanthene dyes, erythrosine B (Ery) and eosin Y (Eos), was studied in a photocatalytic reactor. Photocatalysis was able to degrade 98% of Ery and 73% of Eos and led to 65% of chemical oxygen demand removal. Experiments in buffered solutions at different initial pH values reveal the pH dependence of the process, with better results obtained under acidic conditions due to the electrostatic attraction caused by the opposite charges of TiO_2 (positive) and of anionic dyes (negative). Batch activity tests under methanogenic conditions showed the high toxicity exerted by the dyes even at low concentrations (~85% with initial concentration of 0.3 mmol L^{-1}), but the end products of photocatalytic treatment were much less toxic toward methanogenic bacteria, as detoxification of 85 ± 5% for Eos and 64 ± 7% for Ery were obtained. In contrast, the dyes had no inhibitory effect on the biogenic-carbon biodegradation activity of aerobic biomass, obtained by respirometry. The results demonstrate that photocatalysis combining UV/TiO_2 as a pretreatment followed by an anaerobic biological process may be promising for the treatment of wastewaters produced by many industries.

INTRODUCTION

Photocatalytic systems by irradiation of titanium dioxide (TiO_2) particles are promising advanced oxidation processes (AOP) for degrading several organic compounds (1). The combination of light has been considered more effective as compared to other AOPs, because semiconductors are inexpensive and can easily mineralize various organic compounds without any further additive (2). In the past, many catalysts like TiO_2, ZnO, WO_3, SnO_2, ZrO_2, CeO_2, CdS and ZnS have been used for photocatalytic oxidation of aqueous environmental contaminants (3) but TiO_2 photocatalytic oxidation holds much promise, because of its large surface area (7–50 m^2 g^{-1}), cheap price, insolubility under most conditions, nontoxicity and its favorable redox properties both for oxidation of many organic pollutants and reduction of a number of metal ions in aqueous solution (4,5). TiO_2 catalyst is chemically stable in aqueous media in a large pH range, is photo stable and is able to utilize sunlight and air to produce many reactive species, including the powerful and nonselective oxidant hydroxyl radicals, to destroy organic compounds into harmless species such as CO_2, H_2O and others (6). The only drawback is that TiO_2 possesses certain limitations such as poor absorption of visible radiation and rapid recombination of photogenerated electron/hole pairs (7). UV/TiO_2 process produces less residual pollutants compared to other conventional processes (8). However, the separation of powder from the liquid state and recycling process are troublesome because of the formation of aggregates. Also the depth of penetration of UV light is limited because of strong absorption by both catalyst particles and dissolved organic species. Another disadvantage in water treatment is with regard to its lower quantum efficiency in comparison with gas-phase photocatalysis. The principle reason for this is the smaller availability of oxygen in liquid water and lower mass transport of target chemicals in comparison with air. These difficulties can be overcome by immobilizing the TiO_2 on inert surfaces such as glass beads, activated carbon fiber, cotton material and cement surface. This also opens the possibility of catalyst recycling, reducing the costs associated with the long settling times or filtration methods for its recovery (8–11). The unique requirement can be the catalyst replacement and catalytic regeneration on-site.

During the manufacturing processes, a substantial amount of dyestuff is lost as effluent which causes a major problem for the industry as well as a threat to the environment. Among the various applications reported in literature, the UV/TiO_2 process has been extensively investigated for the destruction of dyestuffs present in dyehouse wastewater (2,5,6). Degradation of xanthene dyes combining TiO_2 in suspension with light has been investigated by other authors (7,12–17). Xanthene dyes have many uses in textile, paper, food, cosmetics, pharmaceuticals, medicine and biological staining, due to superior dyeing and coloring properties. These dyes exhibit poor biodegradability and some of them are toxic (18–21). Likewise, xanthene derivatives hold high microbial inhibition (22). In the present work, inhibitory effect of the xanthene dyes erythrosine B (Ery) and eosin Y (Eos) on biological activity was assessed by batch activity tests using either anaerobic granular biomass or by analysis of respiration inhibition kinetics using biogenic organic matter. A photoreactor combining immobilized TiO_2 and UV light was applied for Er and Eos degradation and the levels of detoxification toward anaerobic and aerobic sludge were assessed.

*Corresponding author email: lucianapereira@deb.uminho.pt (Luciana Pereira)

MATERIALS AND METHODS

Chemicals. The xanthene dyes Ery (95%; C.I. 45430) and Eos (85%; C. I. 45380), were purchased from Sigma Aldrich at the highest analytic grade purity commercially available. The chemical structures are represented in Fig. 1. They have a xanthene ring (A/B/C-ring), which is halogenated either with four bromine groups (Eos) or with four iodine groups (Ery) and a carboxyphenyl ring (D-ring). Stock solutions of 14 mmol L^{-1} were prepared in deionized water.

Photocatalytic reactor. The experimental setup for degradation of xanthene dyes is constituted by a recirculation photocatalytic reactor which consisted of a 37° slanted aluminum plate with a surface working area of 30 × 30 cm^2 (Fig. 2). Prior to each operation, the aluminum surface was inactivated by coating it with a thin layer of PTFE (PTFE AL; Samaro, Villeurbanne, France). A transparent glass sheet covered the reacting chamber to avoid evaporation of the solution. The dye solution (500 mL) in the reservoir was maintained under agitation during the entire operation time and was continuously circulated in the system by a peristaltic pump at a constant flow rate of 130 mL min^{-1}, permitting optimal distribution of the liquid over the catalytic support. The reservoir was open to air to ensure sufficient oxygenation. A thin film flowed from the top of the chamber over a nonwoven fabric made of cellulose fibers on which Tiona PC500 TiO_2 (18 g m^{-2}), UOP 2000 zeolite (2 g m^{-2}) and Snowtex 50 SiO_2 (20 g m^{-2}) were fixed by compression (Ahlstrom, Pont-Evêque, France). Artificial irradiation was provided by two UV lamps emitting light with a wavelength around 365 nm (F15T8, BLB 15W; Duke, Essen, Germany). The lights were positioned in parallel to the reactor. Adsorption measurements of the dyes on immobilized TiO_2 were made using the same setup in the absence of irradiation. Dye degradation only with UV, absence of the fabric containing the TiO_2, was also evaluated. The reactor was washed after every run by circulating deionized water with a few drops of 9% hydrogen peroxide under UV irradiation, so that the immobilized photocatalyst was regenerated (2). Triplicates with the same photocatalyst-loaded fabric were done and the error was ±10%).

Photocatalytic treatment of dye solution. A 500 mL of solution with initial dye concentration of 0.3 mM was prepared in deionized water from a concentrated stock (14 mmol L^{-1}). The pH of final solution was 7.0 for both dyes. In order to study the effect of the pH, new solutions at pH 5.0, 7.0 and 8.0 were made in 100 mmol L^{-1} Britton-Robinson (BR) buffer (100 mmol L^{-1} phosphoric acid, 100 mmol L^{-1} boric acid and 100 mmol L^{-1} acetic acid titrated to the desired pH with 0.5 M NaOH). Color decrease was monitored by spectrophotometry in a 96-well plate reader (ELISA BIO-TEK, Izasa): at selected intervals, samples were withdrawn (1 mL) and diluted in deionized water, or with the same buffer as of the reaction, due to the high absorbance of the dye, even at low concentrations. The visible spectra (300–900 nm) were recorded and dye concentration calculated at λ_{max}. Molar extinction coefficients were calculated for each dye at λ_{max}. ε_{530nm} of ERY was 67 282 mol^{-1} L cm^{-1} and ε_{510nm} of EOS was 60 826 mol^{-1} L cm^{-1}. All the experiments were prepared in triplicate. First order reduction rate constants were calculated with OriginPro 6.1 software (Northampton, MA), applying the exponential decay curve represented by the equation $C_t = C_0 + C_i\, e^{-kt}$, where C_t is the concentration at time t, C_0, the offset, C_i, the concentration at initial time, k is the first-order rate constant (h^{-1}) and t is the time of the experiment. The chemical oxygen demand (COD) was also evaluated during the treatment by using a kit from Hach-Lange (100–2000 mg O_2 L^{-1}—LCK 514). The pH of the solution was controlled using a pH meter (Orion model 720 A).

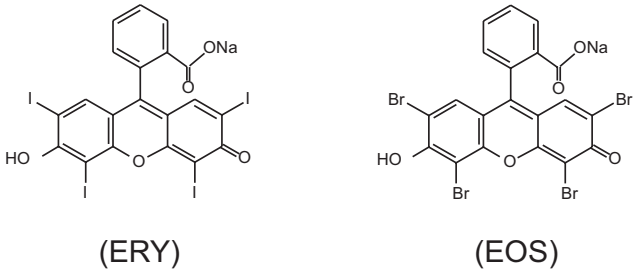

Figure 1. Molecular structure of the xanthene dyes, erythrosine B (Ery) and eosin (Eos).

High-performance liquid chromatography. HPLC analyses were performed in an HPLC (JASCO AS-2057 Plus) equipped with a diode array detector. A C18 reverse phase Nucleodur MNC18 (250 × 4.0 mm, 5 μmol L^{-1} particle size and pore of 100 Å; Machenerey-Nagel, Switzerland)column was used. The following solvent systems were used as mobile phase: solvent A (ACN) and solvent B (sodium acetate buffer, pH 5.3). Compounds were eluted at a flow rate of 0.7 mL min^{-1} and at room temperature, with a linear gradient of mobile phase from 10% to 100% of solvent A, over 15 min, followed by isocratic condition with 100% of solvent A over 10 min. Compounds elution was monitored at λ_{max} of each dye and at 230 nm.

Methanogenic activity experiments. Specific methanogenic activity (SMA) tests were performed in serum bottles of 25 mL working volume of 12.5 mL, containing a buffer solution with 3.05 g L^{-1} sodium bicarbonate and 1 g L^{-1} of Resazurin. Vials were supplemented with 0.4 g anaerobic granular sludge which corresponds to 3.7 ± 1.0 g of volatile suspended solids (VSS) per liter, closed with crimp caps and the headspace was flushed with a mixture of N_2/CO_2 (80/20 vol/vol). The final pH was 7.2 ± 0.2. Following the addition of 0.125 mol L^{-1} Na_2S, under strict anaerobic conditions, the flasks were incubated overnight at 37°C and 120 rpm. After that period, the substrate (3 mol L^{-1} of ethanol) and the dye solution to be tested were added and the flasks were maintained at 37°C and 120 rpm. The pressure was measured every 60 min by using a hand-held pressure transducer able of measuring a pressure variation of ± 2 atm (0–202.6 kPa) with a minimum detectable variation of 0.005 bar, corresponding to 0.05 mL of biogas in a 10 mL headspace. The assay was finished when the pressure remained stable. Methane content of the biogas was measured by gas chromatography using a Chrompack Haysep Q (80–100 mesh) column (Chrompack, Les Ulis, France), with N_2 as carrier gas at 30 mL min^{-1} and a flame-ionization detector. Temperatures of the injection port, column and flame-ionization detector were 120, 40 and 130°C, respectively. The values of methane production were corrected for the standard temperature and pressure conditions. To determine the activities, the values of pressure (calibrated as an analogical signal in mV) were plotted as a function of time and the initial slopes of the methane were calculated. SMA values were determined dividing the initial slope by the VSS content of each vial at the end of the experiment and were expressed in mL CH_4 g_{VSS}^{-1} day^{-1}. Background methane production due to the residual substrate was subtracted. Tests included series containing increasing Ery and Eos concentration, in the range of 0.0625–2 mmol L^{-1}, corresponding to a range of 0.017–0.54 mmol dye per g of volatile solids (VS), to evaluate the effect of the dyes on the biomass activity. The final UV/TiO_2-treated solutions (prepared in deionized water, pH 7) were also tested to assess the potential detoxification by photocatalytic degradation. Two controls were made in the same conditions, one containing only ethanol (no dye) and the other without any substrate or dye (blank assay). All batch experiments were performed in triplicate. The effect of dyes and treated solutions was evaluated by comparing with the control containing only ethanol.

Respiration inhibition kinetics analysis (RIKA). Quantification of the inhibitory effect of the xanthene dyes Ery B and Eos Y on the aerobic biodegradation of biogenic organic matter was done by a pulse respirometric technique, based on the RIKA method, developed by Volskay and Grady (23) and modified by Kong *et al.* (24). The method consisted in the measurement of the Monod kinetic parameters describing the biodegradation of a biogenic-C source (*e.g.* acetate) in the absence (control) and in the presence of determined concentrations of the selected toxicant, in order to quantify the inhibitory effect of the toxicant on the biodegradation of the biogenic-C source.

The aerobic biomass used in the respirometric tests was obtained from a laboratory-scale activated sludge reactor fed acetate as the sole carbon source. Acetate was thus used as biogenic-C source in respirometric tests. Respirometric experiments were made in a 0.5 L transparent acrylic respirometer equipped with magnetic stirring. Air was supplied through a fine bubble aerator placed close to the bottom of the respirometer. Air flow rate was controlled by a mass flow controller (GFC 17S Aalborg). Dissolved oxygen (DO) concentration was measured with a polarographic oxygen probe connected to a DO meter (HI 2400; Hanna Instrument, Portugal) and a computer for data acquisition. The oxygen probe was calibrated before each respirometric experiment. DO readings were automatically corrected for temperature and salt concentration. A 0.5 L test sample of mixed liquor (0.82 ± 0.10 g_{VSS} L^{-1}), collected from the laboratory-scale activated sludge reactor, was placed in the respirometer and aerated for 30 min to reach endogenous respiration prior to the pulse

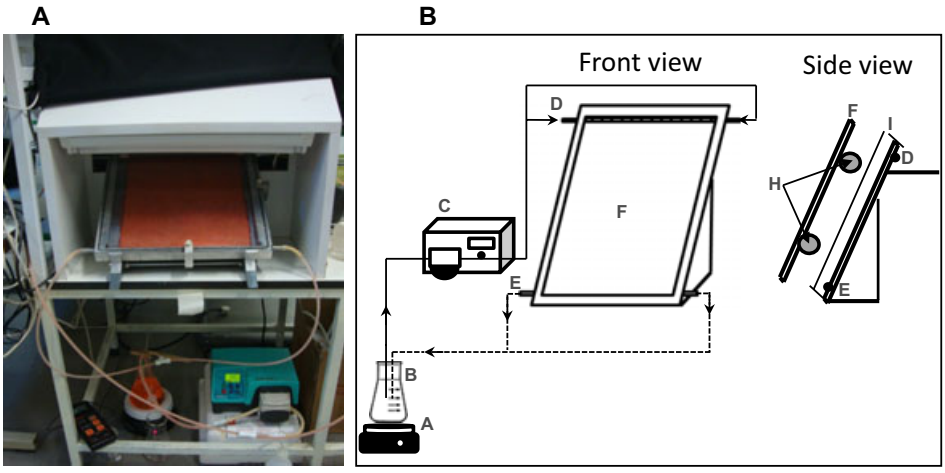

Figure 2. Photography (**A**) and schematic diagram (**B**) of the experimental setup. A = stirring plate; B = reservoir; C = pump; D = feeding from pump; E = flow to reservoir; F = catalyst support; H = lamps; I = glass cover.

respirometric experiments. For each assay one control (absence of toxicant) and two toxicant concentrations (0.2 and 0.4 mM, corresponding to 0.27 and 0.54 mmol g_{VS}^{-1}) were tested. The control experiment consisted in consecutively injecting four pulses of different acetate concentrations in the absence of the toxicant, measuring the initial net exogenous respiration rates. Then, a certain concentration of the toxicant was added and the biomass was exposed to the toxicant for *ca* 30 min. When the exposure time was over, four pulses of different acetate concentrations were injected consecutively and the initial net exogenous respiration rates were measured. Monod curves, representing the relation between the respiration rate and the substrate concentration in the presence and absence (control) of inhibitors, were obtained by plotting the initial exogenous respiration rates *versus* the corresponding acetate concentration. Subsequently, the values of μ_{max} and K_S were estimated by using a nonlinear least squares curve-fitting technique. This way, data on μ_{max} and K_S as a function of inhibitor concentration were provided which could be analyzed further to quantify the effect of the inhibitor on biogenic substrate removal.

RESULTS AND DISCUSSION

Photocatalytic degradation of xanthene dyes

The time course of Ery and Eos photocatalytic degradation was monitored by optical absorption. The UV/visible spectra of initial dye solutions and of 5 and 24 h-treated solutions are illustrated in Fig. 3A,B. Ery showed a maximal absorbance at 530 nm and Eos at 510 nm. A decrease in intensity of the absorbance was observed in the entire spectra of both dyes, indicating their degradation. Concomitant with this decrease, a new absorption band at 230 nm appeared for the Ery-treated solution, demonstrating the generation of new products (Fig. 3A). Similar to the findings of Zhang *et al.* (25), no new absorption bands appeared for the Eos-treated solution, neither in the visible nor in the ultraviolet regions (Fig. 3B). The time course of the enzymatic reaction was also monitored by HPLC where dyes were chromatographically separated from products of the reaction. As observed for Ery, a major peak with retention time, *Rt*, of 10.1 min, corresponding to the dye, decreased over the course of reaction and almost disappeared ($\leq$16%) after 5 h of reaction (Fig. 3C). The emergence of a new peak corresponding to reaction products is observed, with *Rt* of 2.9 min. Eosin chromatograms showed two major peaks at *Rt* of 9.3 and 12.6 min and a minor at *Rt* of 9.7 min, suggesting the presence of contaminants. During the phototreatment, all the peaks decreased and after 24 h, only residual amounts of the substrate at *Rt* 9.3 min (13%) were still in the solution. Similar to that observed by optical spectroscopy, no peaks corresponding to degradation products were detected by HPLC, suggesting total mineralization of the dye.

The curves of dye removal over time, 24 h of treatment, fitted reasonably well by an exponential decay curve, suggesting first-order kinetics (Fig. 3E,F). In spite of the structural similarity of dyes, the rate of degradation was 2.5-fold higher for erythrosine (Table 1). Decolorization degrees of 98 ± 6% and 73 ± 8% were obtained for dye solutions containing erythrosine and eosin, respectively. In the absence of light, decolorization of both dyes was only ~25% and occurred in the first hours of contact, probably due to adsorption. Again, the rate of decolorization was higher, almost the double, for the Ery-containing solution. As observed by HPLC, eosin solution contains more than one compound, which may interfere with the catalysis. Besides, the dye adsorbs onto the surface of TiO_2 by electrostatic attraction and gets mineralized by the OH radicals generated by UV light. Therefore, the adsorption affinity of the target molecule on the catalyst surface may be regarded as a critical step toward efficient photocatalysis. This also explains the higher rate of Ery degradation by UV/TiO_2, once it adsorbs better on TiO_2. In the absence of TiO_2 only *ca* 15% color decrease was obtained for both dyes. The lower degrees of degradation under UV light without the photocatalyst may be regarded with the stability of many dyes to light.

Photocatalytic treatment leads to COD removals of 62% for erythrosine and 65% for eosin (data not shown). Our results agree with other studies reported for this class of dyes as well as for other classes (5,26,27).

Effect of pH on photocatalytic degradation

The photocatalytic degradation of both dyes under investigation was studied at different pH values—5, 7 and 8—as it is an important parameter for the reactions. According to the results, degradation rate for the both model compounds under investigation is strongly influenced by the solution pH. The efficiency of degradation rate was found to be highest at pH 5 and decreases with the increase in pH (Table 1). Final color removal

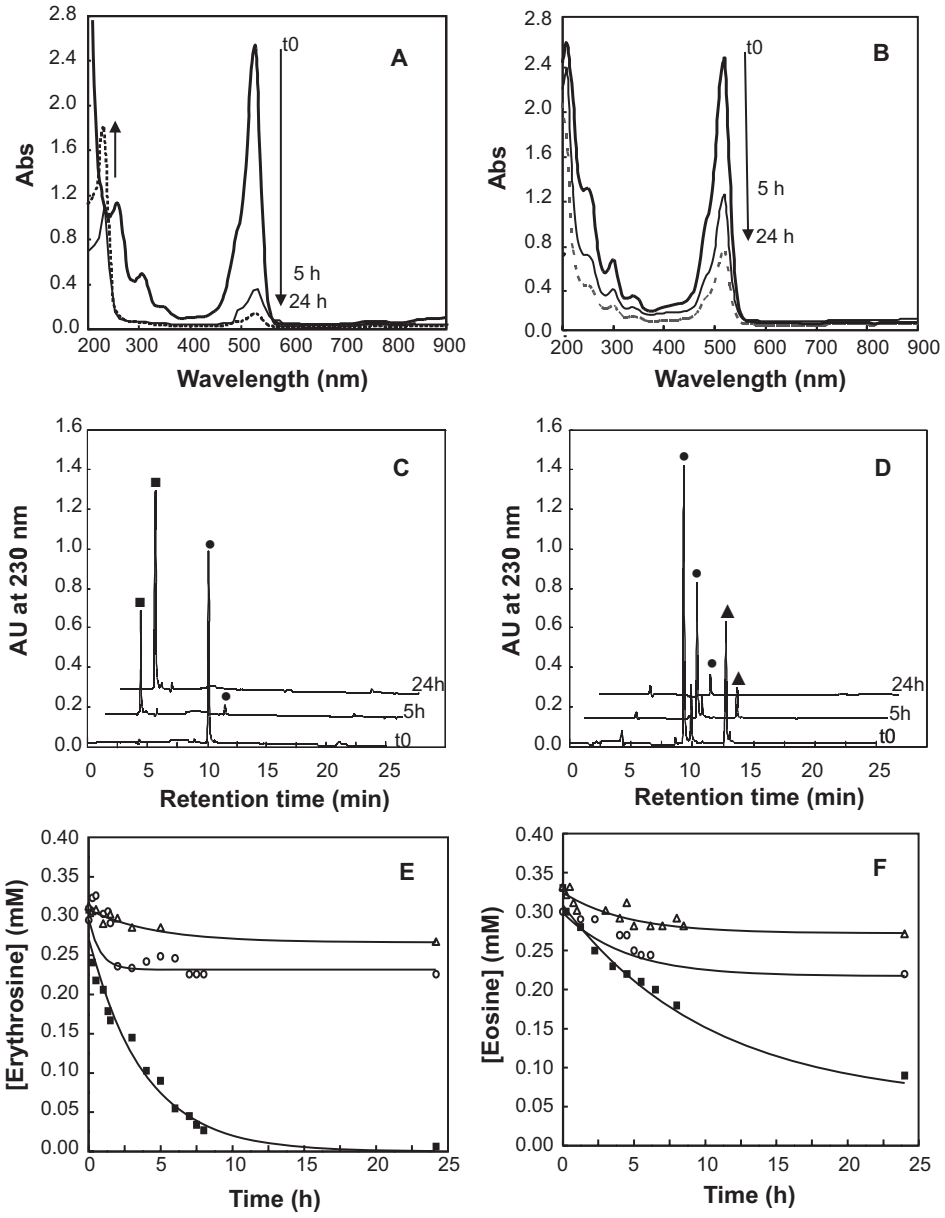

Figure 3. Color decrease as monitored by UV/visible spectroscopy and HPLC and first-order rates of photocatalytic degradation in water solutions, pH 7.0 (A, C and E—Ery; B, D and F—Eos). (●) Dye; (▲) Impurity; (□) Product of Ery degradation; (Δ) only UV light; (○) only TiO_2; (■) combination of UV/TiO_2.

was also obtained under acidic condition, with an Ery decolorization of 73% and Eos decolorization of 58%. At pH 7 and 8, decolorization was only *ca* 20%. The pH of aqueous solution affects the charge of TiO_2. In an aqueous environment it becomes positively charged below the point of zero charge (pH_{pzc}) due to the presence of $TiOH_2^+$ groups and negatively charged above the pH_{pzc}, owing to TiO^- groups (5,6,28). This pH-dependent surface charge shall affect the adsorption of substrates and consequently photocatalytic reactions. Therefore, under acidic pH, TiO_2 is positively charged and, on the other hand, the anionic xanthene dyes are negatively charged in solution, situation favorable to an adsorption mediated by electrostatic attractions, which explains the best results at pH 5. At higher pH values, repulsive forces interact between the negatively charged semiconductor surface and dye anions, thereby making the approach of dye anions on the surface of semiconductor difficult. It results in the decrease in rate of photocatalytic bleaching of dyes. In effect, in buffered solutions, the adsorption of dyes on TiO_2 occurred only at pH 5 (65% for Ery and 43% for Eos). Saquib and Muneer (13) have reported that at lower pH values, the carbonyl group of the xanthene dyes can be in the protonated form and apparently this structural orientation of the molecule is more favored for the attack of the reactive species. However, the visible spectra of Ery and Eos were shown to be independent of the pH, which is indicative of no changes in dye structure and on its protonation/deprotonation equilibrium. Better photocatalytic degradation of Eos under acidic conditions was also reported by other authors (7,13–15,25) as well as for Ery B (16). Comparing both dyes, as observed in the photocatalytic degradation of dye solutions prepared in deionized water, in

Table 1. Degree and rate of 0.3 mmol L^{-1} dye decolorization in the photoreactor (±10%) at different pH conditions.

		UV/TiO_2		TiO_2		UV	
Dye	pH	%	h^{-1}	%	h^{-1}	%	h^{-1}
Ery	**7***	98	0.25	24	0.31	14	0.18
	5†	73	2.28	65	1.89	15	0.21
	7†	24	1.05	nr		nr	
	8†	17	0.30	nr		nr	
Eos	**7***	73	0.10	26	0.18	17	0.23
	5†	46	1.67	43	1.21	nr	
	7†	24	0.76	nr		nr	
	8†	24	0.35	nr		nr	

nr = no dye removal. *Dye solution made in deionized water. †dye solution made in 100 mM Britton-Robinson buffer.

buffered solutions higher rates were also obtained for Ery, except at pH 8, with similar results. According to the literature (29–31), heavy atom substitution can enhance the transition state of the aromatic molecule's singlet-triplet state by increasing the spin-orbit mixing. As the substituted halogen atom becomes heavier, the electronegativity decreases, enhancing the electron-donation capability in the order of H<Cl<Br<I. This is in accordance with our results, the oxidation potential was higher for the dye containing iodine than that containing bromide (I>Br: Ery>Eos). The higher hydrophobicity of Ery as compared with Eos (32) can be also a factor to be considered in the higher and faster adsorption on the fiber that contains the TiO_2-supported fibers and therefore the higher degradation in our studies at pH 5.

The photocatalytic degradation degree in buffered solution at pH 7 was three-fold lower than that obtained in deionized water. The results may be explained by the presence of salts that can compete with the dyes, *i.e.* the competition between the negative inorganic ions and negative charged dyes (33).

Toxicity analysis

Effect of dyes and treated solutions on an anaerobic system. Activity tests using the anaerobic granular biomass were performed to evaluate the cytotoxicity of the xanthene dyes and to compare it with those of their photocatalytic degradation products (Table 2). We found that both dyes have a significant cytotoxic effect on cell activity with inhibition of *ca* 60% with the lowest dye amount tested (0.0625 mmol L^{-1} = 0.052 g L^{-1}) as compared with the control with ethanol (Fig. 4). An increase in the inhibition is visible with the increase in dye concentration, being almost 100% at dye amounts higher than 0.5 mmol L^{-1}. The initial reaction mixture to be treated in the photoreactor, containing 0.3 mmol L^{-1} of dye, exerted similar inhibition on biomass activity for both dyes: 84 ± 4% and 85 ± 2%, for Eos and Ery, respectively. Importantly, the final reaction mixture containing the biotransformation products of eosin is considerably less toxic than the untreated dye solution (only 7 ± 3% activity inhibition). To a lesser extent, lower activity inhibition was also obtained with the final solution containing the erythrosine Photocatalytic degradation by-products (58 ± 5%). Those results allowed us to estimate that the photocatalytic degradation treatment combining UV/TiO_2 leads to a final detoxification of 85 ± 5% for Eos and 64 ± 7% for Ery (Table 2). The high inhibition caused by the xanthene dyes is in agreement with the literature. Bell *et al.* (34) found that, from the 14 different dyes tested, erythrosine caused the highest methanogenic activity inhibition (IC_{50} < 0.2 g L^{-1}). Erythrosine showed a very slight, but statistically significant, mutagenic effect on *Escherichia coli* at a concentration of 5 g L^{-1}. It was found that the xanthene molecule itself was the causative factor and that the substituent groups only modified the effect (35). Lack of mutagenic activity of erythrosine for *Salmonella typhimurium* strains (TA 1535, TA 100, TA 1538, TA 98 and TA 1537) was observed when tested by the Ames test at concentrations ranging from 1 to 10 000 μg per plate with or without metabolic activation system (36).

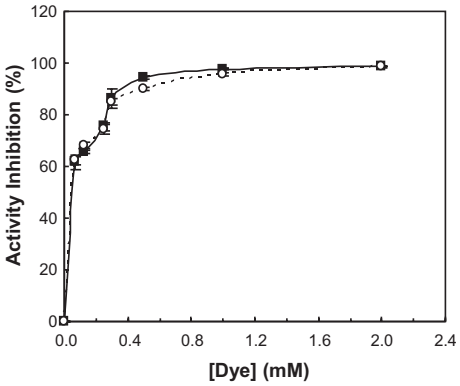

Figure 4. Toxicity of the xanthene dyes as assessed by the inhibitory effect on the anaerobic granular biomass activity with increasing dye concentration (0.0625–2 mmol L^{-1}). (■) Ery; (○) Eos.

Effect of dyes and treated solutions on an aerobic system. Respirometric inhibition kinetic analyses were performed to evaluate the inhibitory effect of the xanthene dyes on the aerobic biodegradation of acetate. Kinetic parameters K_S and μ_{max} obtained with the different tested concentrations of Ery and Eos were compared through one-way ANOVA tests (Statistics 18; SPSS Inc. Package) (Table 3). According to the results, there was no significant effect ($P > 0.05$) of the dyes on the kinetic parameters. Thus, neither one of the tested dyes had an inhibitory effect on the aerobic metabolic activity.

Table 2. Comparison of the activity inhibition exerted by 0.3 mmol L^{-1} of dye before and after photocatalytic degradation treatment and level of detoxification.

	% Activity relative to the control		
Dye	Before treatment	After treatment	Detoxification (%)
Erythrosine	15 ± 1	42 ± 6	64 ± 7
Eosin	16 ± 4	93 ± 6	85 ± 5

Table 3. Aerobic kinetic parameters values obtained through respirometric tests under different dye concentrations, and comparison of means by one-way ANOVA.

		Dye concentration (mmol L^{-1})			ANOVA	
Dye	Parameter	0	1*	2†	$F(2,6)$	P
Ery	K_S (mg L^{-1})	1.9 ± 0.4	1.6 ± 0.5	2.1 ± 0.2	1.2	0.38
	μ_{max} (day^{-1})	1.0 ± 0.1	0.8 ± 0.1	0.9 ± 0.0	4.1	0.08
Eos	K_S (mg L^{-1})	1.7 ± 0.6	1.7 ± 0.2	1.9 ± 0.5	0.2	0.82
	μ_{max} (day^{-1})	0.7 ± 0.1	0.8 ± 0.1	0.9 ± 0.1	4.0	0.08

*0.27 mmol g_{VS}^{-1}. †0.54 mmol g_{VS}^{-1}.

CONCLUSIONS

A photoreactor combining UV/TiO_2 was operated for the photocatalytic degradation of two structurally similar xanthene dyes, erythrosine and eosin. Photocatalysis leads to a high extent of color removal of both dyes. Decolorization could be attributed to two processes—adsorption on TiO_2 and photocatalytic degradation. The treatment was shown to be pH dependent with better results obtained under acidic conditions. The process is advantageous, in comparison with previous published work, as the photocatalyst was immobilized in a nonwoven fabric made of cellulose fibers, with the possibility of being reused and preventing the eco-toxicity impacts associated with the incorrect disposal of free nanoparticles. Activity tests with anaerobic biomass indicated that photocatalysis may be a feasible pretreatment method not only for decolorization and COD removal but also for detoxification of xanthene dye-containing wastewaters. The combination of a photo-pretreatment followed by an anaerobic biological process may be an efficient strategy for the treatment of those wastewaters.

Acknowledgements—This work was supported by a grant of the Romanian National Authority for Scientific Research, CNCS UEFISCDI, project PN-II-ID-PCE-2011-3-0559, contract 265/2011, and the PTDC/AMB/69335/2006 project grants. Luciana Pereira holds a Pos-Doc fellowship (SFRH/BPD/80941/2011), Raquel Pereira holds a fellowship (SFRH/BPD/39086/2007) and Catarina S. Oliveira holds a PhD fellowship (SFRH/BD/32289/2006) from Fundação para a Ciência e Tecnologia.

REFERENCES

1. Thakur, R. S., R. Chaudhary and C. Singh (2010) Fundamentals and applications of the photocatalytic treatment for the removal of industrial organic pollutants and effects of operational parameters: A review. *J. Renew. Sustain. Energy* **2**, 1–37.
2. Khataee, A. R., M. N. Pons and O. Zahraa (2009) Photocatalytic degradation of three azo dyes using immobilized TiO_2 nanoparticles on glass plates activated by UV light irradiation: Influence of dye molecular structure. *J. Hazard. Mater.* **68**, 451–457.
3. Mahmoodi, N. M., M. Arami, N. Y. Limaee and N. S. Tabrizi (2005) Decolorization and aromatic ring degradation kinetics of Direct Red 80 by UV oxidation in the presence of hydrogen peroxide utilizing TiO_2 as a photocatalyst. *Chem. Eng. J.* **112**, 191–196.
4. Chen, J., M. Liu, L. Zhang, J. Zhang and L. Jin (2003) Application of nano TiO_2 towards polluted water treatment combined with electro-photechemical method. *Water Res.* **37**, 3815–3820.
5. Su, Y., L. Deng, N. Zhang, X. Wang and X. Zhu (2009) Photocatalytic degradation of C.I. Acid Blue 80 in aqueous suspensions of titanium dioxide under sunlight. *React. Kin. Catal. Lett.* **98**, 227–240.
6. Dutta, S., S. A. Parsons, C. Bhattacharjee, P. Jarvis, S. Datta and S. Bandyopadhyay (2009) Kinetic study of adsorption Red 198 on TiO_2 surface. *Chem. Eng. J.* **155**, 674–679.
7. Luo, M., D. Bowden and P. Brimblecombe (2009) Removal of dyes from water using a TiO_2 photocatalyst supported on black sand. *Water Air Soil Poll.* **198**, 233–241.
8. Huang, H., G. Huang, H. Chen and Y. Lee (2006) Immobilization of TiO_2 nanoparticles on Fe-filled carbon nanocapsules for photocatalytic applications. *Thin Solid Films* **23**, 1033–1037.
9. Hosseini, S. N., S. M. Borghei, M. Vossoughi and N. Taghavinia (2007) Immobilization of TiO_2 on perlite granules for photocatalytic degradation of phenol. *Appl. Catal. B: Environ.* **74**, 53–62.
10. Yao, S., J. Li and Z. Shi (2010) Immobilization of TiO_2 nanoparticles on activated carbon fiber and its photodegradation performance for organic pollutants. *Particuology* **8**, 272–278.
11. Adams, K. L., D. Y. Lyon and P. J. J. Alvarez (2006) Comparative eco-toxicity of nanoscale. TiO_2, SiO_2, and ZnO water suspensions. *Water Res.* **40**, 3527–3532.
12. Epling, G. A. and C. Lin (2002) Photoassisted bleaching of dyes utilizing TiO_2 and visible light. *Chemosphere* **46**, 561–570.
13. Saquib, M. and M. Muneer (2003) Photocatalytic degradation of two selected textile dye derivatives, Eosine Yellowish and p-Rosaniline, in aqueous suspensions of titanium dioxide. *J. Environ. Sci. Health Part A—Toxic/Hazard. Subst. Environ. Eng.* **A38**, 2581–2598.
14. Bandara, J., S. S. Kuruppu and U. W. Pradeep (2006) The promoting effect of MgO layer in sensitized photodegradation of colorants on TiO2/MgO composite oxide. *Coll. Surf. A: Physicochem. Eng. Aspects* **276**, 197–202.
15. Uddin, M. M., M. A. Hasnat, A. J. F. Samed and R. K. Majumdar (2007) Influence of TiO_2 and ZnO photocatalysts on adsorption and degradation behaviour of erythrosine. *Dyes Pigm.* **75**, 207–212.
16. Yin, M., Z. Li, J. Kou and Z. Zou (2009) Mechanism investigation of visible light-induced degradation in a heterogeneous TiO_2/Eosin Y/Rhodamine B system. *Environ. Sci. Technol.* **43**, 8361–8366.
17. Jain, R. and S. Sikarwar (2010) Semiconductor-mediated photocatalyzed degradation of erythrosine dye from wastewater using TiO_2 catalyst. *Environ. Technol.* **31**, 1403–1410.
18. Itoh, K. and C. Yatome (2004) Decolorization and degradation of xanthene dyes by a white rot fungus, *Coriolus versicolor*. *J. Environ. Sci. Health Part A—Toxic/Hazard. Subst. Environ. Eng.* **39**, 2383–2389.
19. Tsuda, S., M. Murakami, N. Matsusaka, K. Kano, K. Taniguchi and Y. F. Sasaki (2001) DNA damage induced by red food dyes orally administered to pregnant and male mice. *Toxicol. Sci.* **61**, 92–99.
20. Dadal, A. and M. K. Poddar (2009) Short-term erythrosine B-induced inhibition of the brain regional serotonergic activity suppresses motor activity (exploratory behavior) of young adult mammals. *Pharmacol. Biochem. Behav.* **92**, 574–582.
21. Mizutani, T. (2009) Toxicity of xanthene food dyes by inhibition of human drug-metabolizing enzymes in a noncompetitive manner. *J. Environ. Public Health* **2009**, 953952 (9 pp), DOI:10.1155/2009/953952.
22. Wang, H., L. Lu, S. Zhu, Y. Li and W. Cai (2006) The phototoxicity of xanthene derivatives against *Escherichia coli*, *Staphylococcus aureus*, and *Saccharomyces cerevisiae*. *Curr. Microbiol.* **52**, 1–5.
23. Volskay, V. and C. Grady (1990) Respiration inhibition kinetic analysis. *Water Res.* **24**, 863–874.
24. Kong, Z., P. Vanrolleghem and W. Verstraete (1994) Automated respiration inhibition kinetics analysis (ARIKA) with a respirographic biosensor. *Water Sci. Technol.* **30**(4), 275–284.
25. Zhang, F., J. Zhao, T. Shen, H. Hidaka, E. Pelizzetti and N. Serpone (1998) TiO_2-assisted photodegradation of dye pollutants II. Adsorption and degradation kinetics of eosin in TiO_2 dispersions under visible light irradiation. *Appl. Catal. B: Environ.* **15**, 147–156.
26. Parida, K. M., N. Sahu, N. R. Biswal, B. Naik and A. C. Pradhan (2008) Preparation, characterization, and photocatalytic activity of sulfate-modified titania for degradation of methyl orange under visible light. *J. Coll. Interf. Sci.* **318**, 231–237.
27. Rego, E., J. Marto, P. S. Marcos and J. A. Labrinch (2009) Decolouration of Orange II solutions by TiO_2 and ZnO active layers screen-printed on ceramic tiles under sunlight irradiation. *Appl. Catal. A: Gen.* **355**, 109–114.
28. Park, H. and W. Choi (2005) Photocatalytic reactivities of Nafion-coated TiO_2 for the degradation of charged organic compounds under UV or visible light. *J. Phys. Chem. B* **109**, 11667–11674.
29. Bhowmik, B. B. and P. Ganguly (2005) Photophysics of xanthene dyes in surfactant solution. *Spectroc. Acta, Part A* **61**, 1997–2003.
30. Zhang, X. F., Q. Liu, H. Wang, Z. Fu and F. Zhang (2008) Photophysical behavior of lipophilic xanthene dyes without the involvement of photoinduced electron transfer mechanism. *J. Photochem. Photobiol. A: Chem.* **200**, 307–313.
31. Lee, S. H., D. H. Nam and C. B. Park (2009) Screening xanthene dyes for visible light-driven nicotinamide adenine dinucleotide regeneration and photoenzymatic synthesis. *Adv. Syn. Catal.* **351**, 2589–2594.
32. Majima, E., N. Yamaguchi, H. Chuman, Y. Shinohara, M. Ishida, S. Goto and H. Terada (1998) Binding of the fluorescein derivative eosin Y to the mitochondrial ADP/ATP carrier: Characteriza-

tion of the adenine nucleotide binding site. *Biochemistry* **37**, 424–432.
33. Guillard, C., E. Puzenat, H. Lachheb, A. Houas and J.-M. Herrmann (2005) Why inorganic salts decrease the TiO_2 photocatalytic efficiency. *Int. J. Photoen.* **7**, 1–9.
34. Bell, J., J. J. Plum, C. A. Buckley and D. C. Stuckey and (2000) Treatment and decolorization of dyes in an anaerobic baffled reactor. *J. Environ. Eng.* **126**(11), 1026–1032.
35. Lück, H., P. Wallnofer and H. Bach (1963) Lebenmittel-zusatzstoffe und mutagene Wirkung. VII. Mittellung. Prüfung einiger Xanthen-Farbstoffe auf mutagene Wirkung an *E. coli*. *Path. Microbiol. (Basel)* **26**, 206–224.
36. Brown, J. P., G. W. Roehm and R. J. Brown (1978) Mutagenicity testing of certified food colours and related azo, xanthene and triphenylmethane dyes with the *Salmonella* microsome system. *Mutat. Res.* **56**, 249–271.